Molecular Cell, Vol. 20, 289–300, October 28, 2005, Copyright ©2005 by Elsevier Inc. DOI 10.1016/j.molcel.2005.08.034

ERp29 Triggers a Conformational Change in Polyomavirus to Stimulate Membrane Binding

Brian Magnuson,[1,4] Emily K. Rainey,[1,4] Thomas Benjamin,[2] Mikhail Baryshev,[3] Souren Mkrtchian,[3] and Billy Tsai[1,*]
[1]Department of Cell and Developmental Biology
University of Michigan Medical School
4643 Medical Sciences II
1335 East Catherine Street
Ann Arbor, Michigan 48109
[2]Department of Pathology
Harvard Medical School
Boston, Massachusetts 02115
[3]Division of Molecular Toxicology
Institute of Environmental Medicine
Karolinska Institutet
Nobels väg 13
Stockholm
Sweden

Summary

Membrane penetration of nonenveloped viruses is a poorly understood process. We have investigated early stages of this process by studying the conformational change experienced by polyomavirus (Py) in the lumen of the endoplasmic reticulum (ER), a step that precedes its transport into the cytosol. We show that a PDI-like protein, ERp29, exposes the C-terminal arm of Py's VP1 protein, leading to formation of a hydrophobic particle that binds to a lipid bilayer; this reaction likely mimics initiation of Py penetration across the ER membrane. Expression of a dominant-negative ERp29 decreases Py infection, indicating ERp29 facilitates viral infection. Interestingly, cholera toxin, another toxic agent that crosses the ER membrane into the cytosol, is unfolded by PDI in the ER. Our data thus identify an ER factor that mediates membrane penetration of a nonenveloped virus and suggest that PDI family members are generally involved in ER remodeling reactions.

Introduction

Viruses must overcome numerous host-cell barriers to deliver their nucleic acid into the cytosol or nucleus to cause infection. One critical barrier is the complex membranous system surrounding and residing within the host cell. Depending on the penetration site (i.e., the plasma membrane or an intracellular membrane), viruses have devised unique strategies to breach this barrier (Smith and Helenius, 2004). These strategies are dictated by the nature of the viral structure itself along with the particular cellular conditions (e.g., pH, redox, and cellular factors) that exist at the penetration site. A critical structural feature regulating their membrane transport process is the presence or absence of an envelope surrounding the virus.

Penetration of enveloped viruses across a membrane has been well characterized; virally encoded hydrophobic "fusion peptides" embedded within the envelope become exposed in response to a triggering event, promoting the fusion of the viral and cellular membrane (Poranen et al., 2002). Consequently, the viral nucleoprotein complex is delivered de facto across the cellular membrane. For example, influenza virus is first taken up by endocytosis into endosomal compartments where the low pH environment triggers the exposure of a hydrophobic peptide buried within the viral membrane (Skehel and Wiley, 2000); the hydrophobic peptide stimulates fusion of the viral and endosomal membrane, thereby delivering the viral nucleocapsid into the cytosol.

However, nonenveloped viruses such as the murine polyomavirus (Py) and SV40 must have a fundamentally different membrane penetration mechanism than that of enveloped viruses because nonenveloped viruses lack a lipid bilayer. Although direct experimental data is sparse (Fricks and Hogle, 1990; Chandran et al., 2002), these viruses are thought to cross biological membranes by interacting with cellular cues (e.g., receptors, proteases, chaperones) that impart conformational changes and render the viruses hydrophobic. The hydrophobic viral particles then penetrate the membrane by locally inducing "pores" in the lipid bilayer. The physiological factors that induce the conformational changes to the nonenveloped viruses and how the remodeling reactions facilitate their membrane penetration have been poorly characterized to date.

We focused our study on the molecular mechanisms by which Py penetrates a cellular membrane. Structurally, the Py capsid is made up of 72 pentamers of the major structural protein VP1, with each VP1 extending its long C-terminal arm to adjacent pentamers to stabilize interpentamer interactions (Stehle et al., 1994). Each VP1 pentamer also binds to an internal VP2 or VP3 protein through hydrophobic interactions (Chen et al., 1998). The VP2 and VP3 proteins overlap in sequence and differ only at their N terminus, where the longer VP2 protein contains a myristic acid (Streuli and Griffin, 1987). The viral DNA is in turn packaged within the virus.

To infect cells, Py and SV40 bind to glycolipid receptors called ganglioside GD1a and GM1, respectively, on the host cell's plasma membrane (Tsai et al., 2003; Gilbert and Benjamin, 2004). The viruses are subsequently transported to the endoplasmic reticulum (ER) lumen (Kartenbeck et al., 1989; Pelkmans et al., 2001; Tsai et al., 2003). Transport to the ER is essential, as treatment of cells with brefeldin A (a drug that interferes with trafficking between the ER and Golgi) blocks Py and SV40 infection (Richards et al., 2002; Gilbert and Benjamin, 2004). From this compartment, these viruses are believed to penetrate the ER membrane in order to reach the cytosol (Norkin et al., 2002; Pelkmans and Helenius, 2003). Although it is possible that Py is transported di-

*Correspondence: btsai@umich.edu
[4]These authors contributed equally to this work.

rectly from the ER into the nucleus (i.e., the ER membrane is continuous with the nuclear membrane), evidence shows that SV40 is transported into the cytosol prior to reaching the nucleus (Nakanishi et al., 1996). Subsequent transport of the virus to the nucleus enables transcription and replication of the viral DNA, leading to lytic infection or cell transformation.

Although the molecular mechanism of Py transport from the ER into the cytosol remains undefined, important insights may be drawn from other pathogens that hijack cellular factors in their efforts to breach the ER membrane. The best example is the transport of cholera toxin (CT) across the ER membrane. To intoxicate cells, CT travels from the plasma membrane to the ER, where it is unfolded by the ER oxido-reductase protein disulfide isomerase (PDI) (Tsai et al., 2001). This step prepares the toxin for transport across an ER membrane channel (Schmitz et al., 2000) to reach the cytosol, where it exerts its cytotoxic effect. We postulate that Py, analogous to CT transport, would experience a conformational change in the ER to initiate its transport across the ER membrane. However, because Py is significantly larger than CT (450 Å versus 60 Å in diameter), Py is unlikely to pass though a protein-conducting channel in the ER membrane. How the virus is transported across the ER membrane subsequent to the structural changes is completely unknown.

Here, we clarify the early stages of Py's membrane transport process by identifying ERp29, an ER resident protein structurally related to PDI (Mkrtchian et al., 1998), as a factor essential in exposing the VP1 C-terminal arm in the ER. This reaction leads to the formation of a hydrophobic viral particle that binds to a lipid bilayer, a step that may prepare the virus for transport directly across the ER membrane. In the intact cell, overexpression of the dominant-negative ERp29 N-terminal domain (NTD) that blocked the Py conformational change in vitro concomitantly decreased Py infection, implicating ERp29 as a critical component in the viral infection pathway. Our data thus identify an ER factor that mediates membrane penetration of a nonenveloped virus and suggest that PDI family members are generally involved in ER remodeling reactions.

Results

ER Activity Triggers a Conformational Change in Py

To determine whether the Py virion undergoes a conformational change in the ER, intact Py particles were incubated with an extract containing ER lumenal proteins derived from dog pancreas (henceforth referred to as lumenal extract) under conditions similar to those previously defined for the study of CT unfolding (Tsai et al., 2001). Conformational changes were detected by monitoring the pattern of digestion products after treatment with trypsin. When particles of the small plaque RA strain of Py were incubated with trypsin, partial digestion of the VP1 protein was seen (Figure 1A, compare lane 2 to lane 1). Incubation of the virus with the reducing agent dithiothreitol (DTT) and the calcium chelator EGTA generated a specific band of approximately 40 kDa (called "VP1a") after trypsin addition (Figure 1A, compare lane 8 to lane 7). In contrast, when we incubated Py in the presence of DTT, EGTA, and a lumenal extract followed by trypsin addition, a distinct band of approximately 38 kDa (named "VP1b") appeared (Figure 1A, compare lane 16 to lane 15). This fragment was also seen when Py was incubated with a lumenal extract and either DTT (Figure 1A, lane 12) or, to a lesser extent, EGTA alone (Figure 1A, lane 14). Incubation of the more tumorigenic large plaque PTA strain of Py with a lumenal extract, DTT, and EGTA followed by trypsin addition also induced the appearance of the VP1b peptide (Figure 1B, compare lane 8 to lane 4). Because a mouse is Py's natural host, we tested whether exposure of Py virions to an ER lumenal extract derived from mouse pancreas generates the VP1b fragment and found that it does (Figure 1C, lane 3). We conclude that an ER activity efficiently alters the conformation of Py VP1.

To identify the trypsin-cleavage site in VP1 that generates the VP1b fragment, VP1 and VP1b were isolated and subjected to mass-spectrometry. A C-terminal tryptic fragment (residues 353–368) is absent in VP1b. No tryptic fragments were found to match the N terminus of either VP1 or VP1b. Due to the many lysine and arginine residues at the N terminus of VP1, tryptic fragments generated from this region would be very small and, hence, undetectable using mass-spectrometry. These findings indicate that ER activity minimally exposes the VP1 C-terminal arm. Whether the N terminus of VP1 is also exposed remains unknown. Because X-ray structural studies previously demonstrated that the VP1 C-terminal arms invade neighboring pentamers to stabilize the virion structure (Figure 1D, Stehle et al., 1994), externalization of the C-terminal arm by the ER activity would likely destabilize the virus.

The ER activity is energy independent, as the VP1b fragment was generated in the absence of ATP (Figure 2, compare lane 4 to lane 6), but it is heat-labile (Figure 2, lane 8). Confirming our hypothesis that the structural change experienced by Py is an ER-specific event, the activity was present in a lumenal, but not a cytosolic, extract (Figure 2, compare lane 10 to lanes 6 and 4). The lumenal extract was not measurably contaminated with cytosolic proteins or vice versa, as the ER protein PDI was present only in the lumenal extract and the cytosolic protein Hsp90 only in the cytosolic extract (Figure 2, compare lane 11 to lane 12).

ERp29 Triggers the Conformational Change in Py

Based on initial studies showing that ER activity was not retained by a concanavalin A column and that it was retained by a strong, but not a weak, anion exchange column, we devised a purification scheme outlined in Figure 3A (solid arrows, see Experimental Procedures). By using this protocol, we found three fractions (i.e., fractions 8, 9, and 10) that generated a single VP1b fragment (Figure 3B, top, lanes 3–5). Although Coomassie staining identified approximately seven distinct protein bands in these fractions (Figure 3B, bottom), only two protein levels peaked within the fractions, one at approximately 29 kDa (**) and the other at 31 kDa (*).

To identify these two proteins, the 29 kDa and 31 kDa bands in fraction eight were excised and subjected to mass-spectrometry. The 29 kDa protein band was iden-

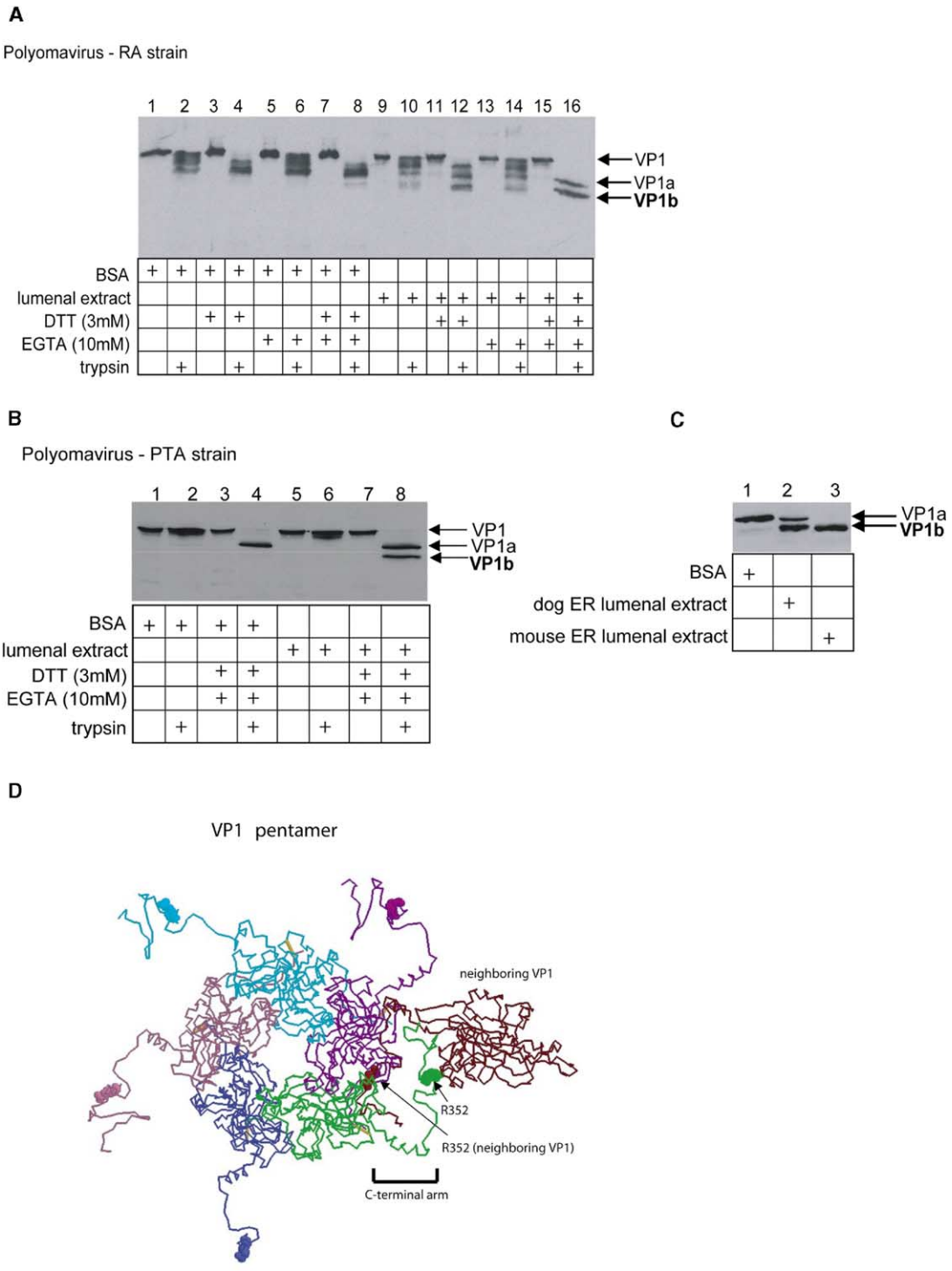

Figure 1. ER Activity Triggers a Conformational Change in Py

(A) Py (RA strain) was incubated with a control protein (bovine serum albumin, BSA) or a lumenal extract with or without DTT and/or EGTA followed by trypsin addition. Samples were analyzed by SDS-PAGE and immunoblotted with VP1 antibody.

(B) As in (A) except the Py PTA strain was used.

(C) As in (A) except a lumenal extract derived from mouse (instead of dog) microsomes was used.

(D) Mass-spectrometry demonstrated that a C-terminal tryptic fragment (residues 353–368) in VP1 is absent in VP1b. Thus, the C-terminal arm of VP1 is exposed by ER activity. The position of R352 is highlighted in the existing structure of Py VP1 pentamer (PDB number 1sid) to pinpoint the region of the virus that likely is exposed.

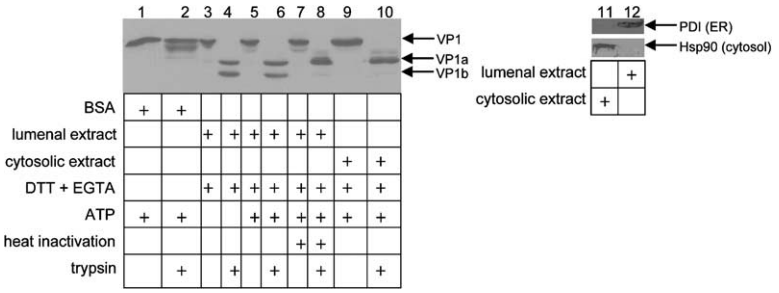

Figure 2. ER Activity Is Heat-Labile and Energy Independent

Py (RA) was incubated with BSA, a lumenal extract (with or without heat inactivation), or a cytosolic extract in the presence of DTT/EGTA and ATP (where indicated), followed by trypsin addition. Samples were analyzed as in Figure 1. The lumenal and cytosolic extracts were immunoblotted with antibodies against PDI and Hsp90.

tified as ERp29 (Figure 3C, left), an ER-resident protein that structurally belongs to the PDI family. An antibody against rat ERp29 confirmed the identity of the 29 kDa protein (Figure 3C, right). Mass-spectrometry did not identify the 31 kDa band directly, and it was therefore subjected to N-terminal sequencing. Sequence analysis showed the first 10 amino acids of the 31 kDa protein to be similar to a predicted 31 kDa mammalian ER-resident protein (Clissold and Bicknell, 2003). Because the 31 kDa protein contains two thioredoxin domains, it also belongs to the PDI family.

To determine whether ERp29 is required to trigger the conformational change in Py virions, we immunodepleted ERp29 from the lumenal extract (Figure 4A, left bottom panel, compare lane 2 to lane 3) and showed that exposure of Py virions to the depleted extract did not generate VP1b (Figure 4A, left top panel, compare lane 2 to lane 3). To establish the specificity of this immunodepletion experiment, we immunodepleted PDI and Ero1 (two ER factors previously shown to unfold CT) from the extract (Figure 4A, right bottom panels) and found that exposure to the depleted extracts generated VP1b to the same extent as exposure to the untreated extracts (Figure 4A, right top panel, compare lanes 6 and 7 to lane 5). ERp29 is also required to trigger the conformational change in particles of the Py PTA strain (Figure 4B, compare lane 3 to lane 2). Thus, ERp29 and/or associated factors expose the VP1 C-terminal arm.

To determine if overexpression of ERp29 stimulates activity, we transfected a construct encoding rat ERp29 into NIH 3T6 cells, harvested the extracts, and tested them for the ability to generate the VP1b peptide. We found a 3T6 cell extract overexpressing ERp29 (Figure 4C, second panel from top, compare lane 2 to lane 1) enhanced the appearance of the VP1b fragment when compared to a control cell extract (Figure 4C, top panel, compare lane 2 to lane 1); the presence of a small amount of VP1b in the control is likely due to endogenous ERp29. The increased activity is not likely to come from upregulation of other ER-resident factors, as the level of PDI, ERp57, ERp72, and Bip did not increase in the extract from ERp29 overexpressing cells (Figure 4C, bottom four panels, compare lane 2 to lane 1). Neither a bacteria extract containing ERp29 nor a purified, bacterially expressed, and His-tagged ERp29 protein alone or in combination with an ERp29-depleted lumenal extract induced the formation of the VP1b peptide (Figure 4C, compare lane 5 to lane 4 and compare lanes 10 and 9 to lane 7). Moreover, a 3T6 cell lysate overexpressing the p31 PDI-like protein (Figure 3C) did not increase VP1b formation compared to a control extract (not shown). These data indicate that ERp29 is active when expressed in mammalian cells, but not in bacteria, and, along with the immunodepletion data, establish ERp29 as a crucial factor that exposes the C-terminal arm of VP1.

Based on sequence analysis, ERp29 can be divided into an N-terminal thioredoxin domain (NTD) and a C-terminal domain (CTD), with the former shown to mediate homodimerization (Liepinsh et al., 2001). If the ERp29 homodimer represents active ERp29, we reasoned that addition of ERp29 NTD may disrupt the active form of ERp29 and inhibit its activity. To test this hypothesis, we purified recombinant His-tagged ERp29 NTD and CTD from bacteria (Figure 4D, lanes 1 and 2). By themselves, neither the NTD nor the CTD generated the VP1b fragment (Figure 4D, lanes 5 and 10). We found, however, that addition of ERp29 NTD to the lumenal extract inhibited the generation of VP1b (Figure 4D, compare lane 7 to lane 6). As a control, addition of ERp29 CTD to the lumenal extract did not prevent VP1b formation (Figure 4D, compare lane 12 to lane 11). These findings provide independent evidence for the role of ERp29 in mediating the conformational change in polyoma virions and demonstrate that the ERp29 NTD has a dominant-negative effect in the reaction.

ERp29 Stimulates Py to Bind Liposomes

We hypothesize that due to its large size, Py penetrates directly across the ER membrane lipid bilayer instead of across a protein-conducting channel. To do so, the virus would be rendered hydrophobic after experiencing a conformational change in the ER, allowing it to bind to the lumenal side of the ER membrane and to initiate transport of the virus particle into the cytosol. We therefore tested whether the change triggered by ERp29 causes Py virions to associate with liposomes. Py particles were first incubated with a lumenal extract to induce the conformational change. Biotinylated liposomes bound to Streptavidin-coated magnetic beads were added to the samples. Each sample was then transferred to a magnetic apparatus to sediment the liposomes and any membrane bound materials. The unbound material remained in the supernatant and was separated from the pelleted fraction. The amount of Py in the pellet (i.e., virus that bound to the liposomes) versus the supernatant fraction (i.e., virus that did not bind to the liposomes) was analyzed by sodium dodecyl-sulfate-polyacrylamide gel electrophoresis (SDS-

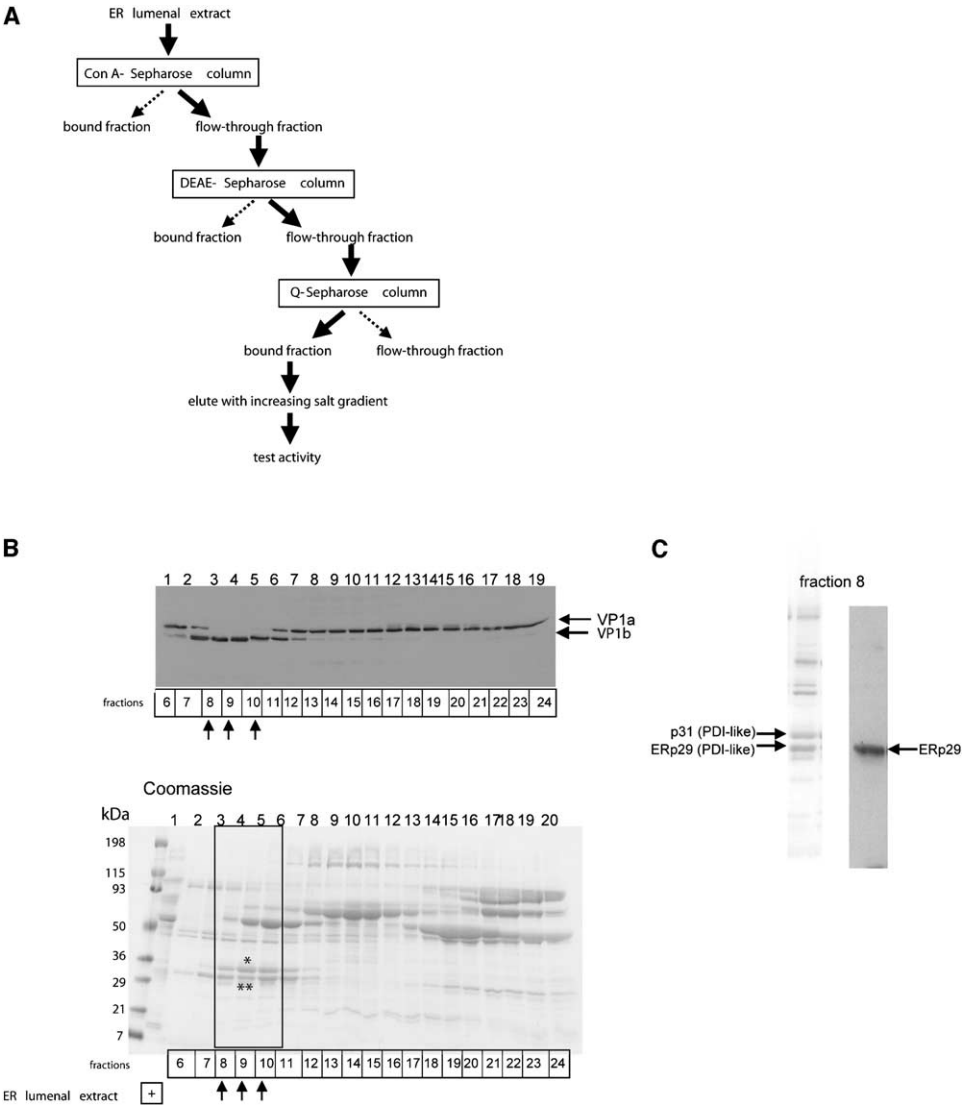

Figure 3. ER Activity Fractionation

(A) Based on initial studies, a strategy was developed to identify ER activity, with the expected activity fractionation pattern indicated by solid arrows.

(B) (upper) The unbound lumenal proteins from Con A- and DEAE-Sepharose columns were bound to a Q-Sepharose column and eluted with a continuous salt gradient. Activity in each fraction was analyzed as in Figure 1. Fractions (lower) were analyzed for their protein content by reducing SDS-PAGE followed by Coomassie staining. Asterisk (*) indicates the 31 kDa protein and (**) indicates the 29 kDa protein.

(C) (left) The 29 and 31 kDa protein bands in fraction 8 were excised and subjected to mass-spectroscopy analysis or N-terminal sequencing, respectively. The 29 kDa protein was identified as ERp29, an ER resident protein, whereas the 31 kDa protein is an uncharacterized ER-resident thioredoxin-containing protein. An antibody (right) against rat ERp29 confirmed the identity of the 29 kDa protein.

PAGE) followed by immunoblotting with a VP1 antibody (Figure 5). Under these conditions, we found that in the absence of liposomes, the VP1 protein of Py incubated with either BSA or a lumenal extract remained in the supernatant (Figure 5A, compare lane 1 to lane 2 and lane 3 to lane 4). In the presence of liposomes, however, a substantial portion of the VP1 incubated with a lumenal extract was in the pellet (Figure 5A, compare lane 8 to lane 7 and lane 6 to lane 5). The virus-liposome interaction was resistant to high salt conditions (not shown), suggesting that binding of Py to the membrane is hydrophobic and not electrostatic. We conclude that an ER activity stimulated the VP1 proteins to bind to a lipid bilayer, presumably as a consequence of increased particle hydrophobicity.

In addition to VP1, both the internal proteins VP2 and VP3 were transferred to the liposomes after exposure to a lumenal extract, but BSA was not (Figure 5B, compare lane 4 to lane 2). These results suggest that the entire virus binds liposomes. To determine whether the membrane-associated virus is bound to the surface of the liposomes or penetrates its interior, the samples were treated with proteinase K. This treatment completely digested the liposome bound VP1, VP2, and VP3 (Figure 5B, lane 8). It is possible that the membrane-associated virus penetrated the liposome and ruptured

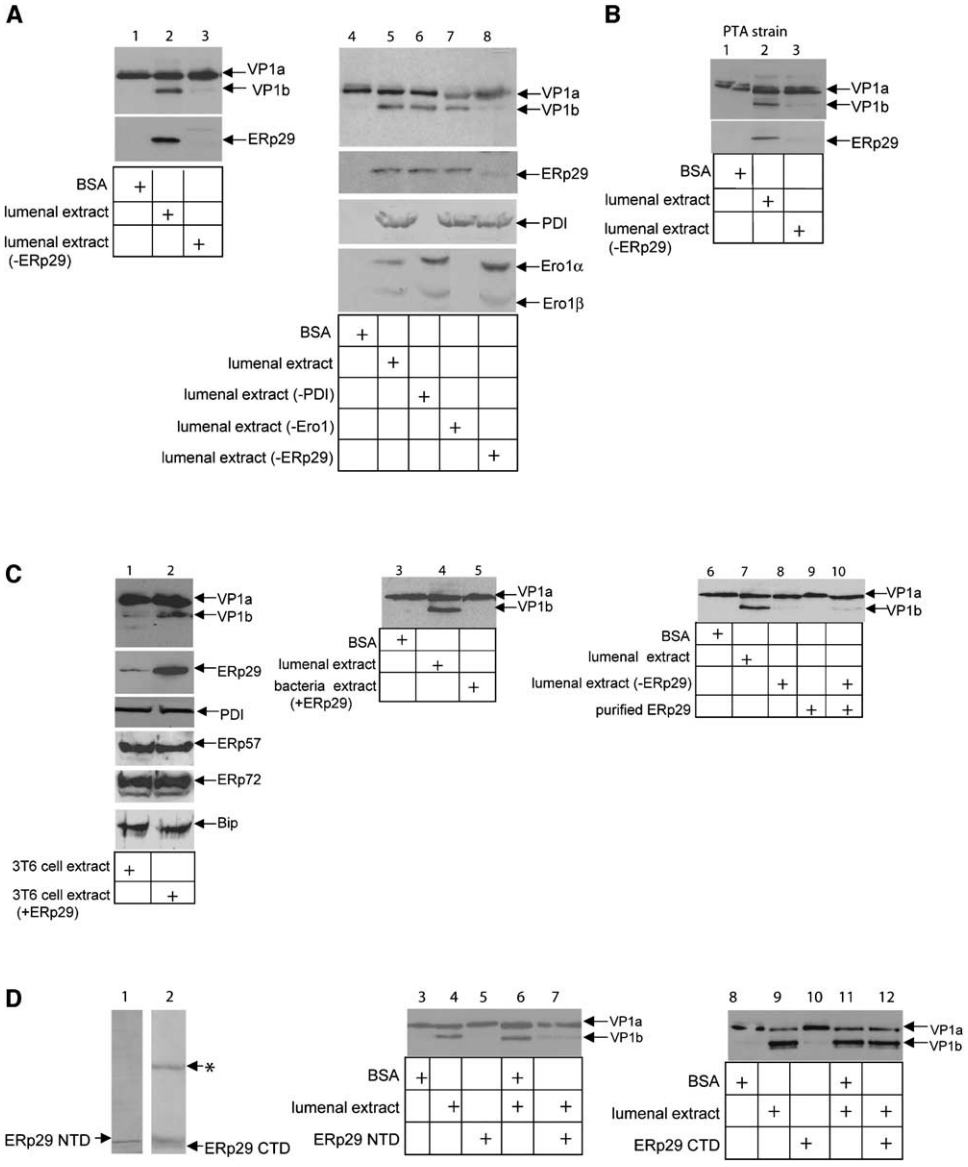

Figure 4. ERp29 Triggers the Conformational Change in Py

(A) (left) The ability of an ERp29-depleted extract to induce VP1b formation was analyzed as in Figure 1. Samples were also immunoblotted with an antibody against ERp29. (Right) A PDI- and an Ero1-depleted extract were tested for their ability to induce VP1b formation. Samples were also immunoblotted with an antibody against ERp29, PDI, and Ero1 (α/β).

(B) As in (A) except Py PTA strain was used in the reaction.

(C) (left) Nontransfected and ERp29-transfected 3T6 cell extracts were tested for activity. The levels of ERp29, PDI, ERp57, ERp72, and Bip in the lysates were analyzed by immunoblotting with the appropriate antibodies. (Middle) Bacterial extract containing His-tagged ERp29 was tested for activity. (Right) Purified bacterially expressed ERp29 incubated with or without an ERp29-depleted extract was tested for activity.

(D) (left) His-tagged ERp29 NTD and CTD were expressed in bacteria and purified. Asterisk (*) indicates an unidentified protein. (Middle) Py was incubated with BSA, a lumenal extract, the NTD, a lumenal extract containing BSA, or a lumenal extract containing the NTD, and activity was assessed as in Figure 1. (Right) As per the middle panel, except the CTD was used instead of the NTD.

the membrane as a consequence, allowing proteinase K to enter. To verify the integrity of the liposome, we incorporated a His-tagged ERp29 protein into the liposomes and tested ERp29's resistance to proteinase K digestion. In the absence of the lumenal extract and Py, a partial degradation of the ERp29 protein was seen (Figure 5B, compare lane 10 to lane 9), suggesting that the ERp29 protein was largely protected by the liposome. Addition of Triton X-100 rendered the protease-resistant species sensitive to degradation (Figure 5B, lane 11), indicating that the liposome protected the ERp29 protein. However, in the presence of Py and the lumenal extract, the liposome-incorporated ERp29 protein did not become more sensitive to protease digestion (Figure 5B, compare lane 12 to lane 10), suggesting that the liposome remained intact in the presence of Py

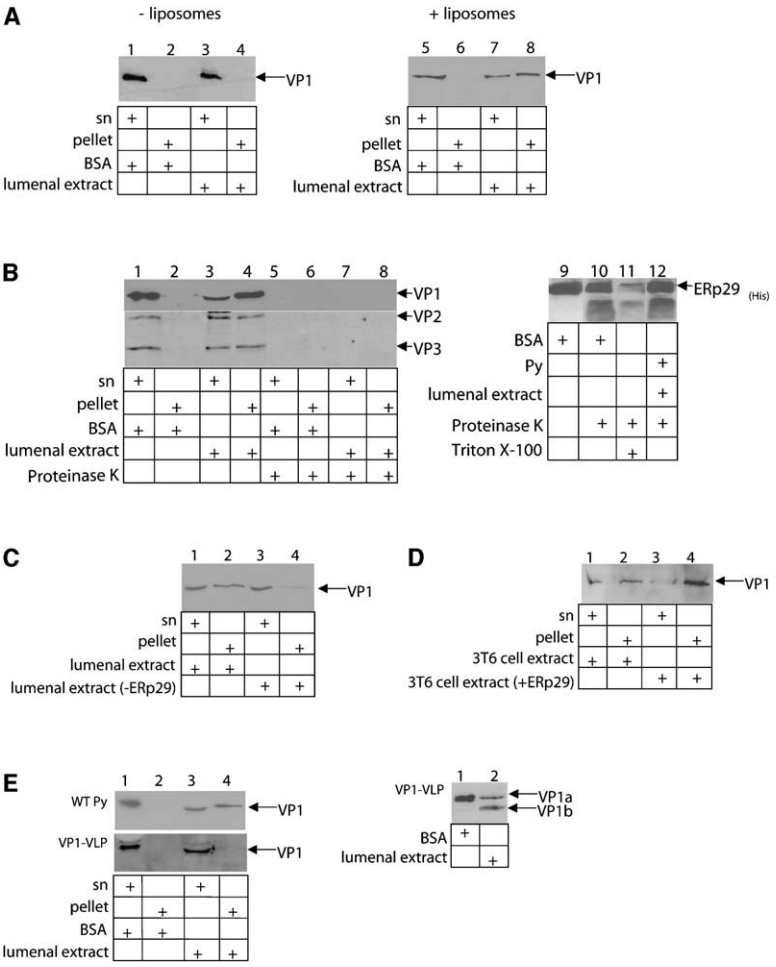

Figure 5. ERp29 Induces Py to Bind to Membranes

(A) Py was incubated with BSA or a lumenal extract followed by the addition of biotinylated-liposomes (where indicated) bound to Streptavidin-coated magnetic beads. Samples were transferred to a magnetic apparatus to separate the membrane bound (pellet) from the membrane unbound (SN) fractions. The samples were analyzed by SDS-PAGE followed by immunoblotting with an antibody against VP1.

(B) (left) As in (A) except where indicated. Samples were treated with proteinase K. The samples were also immunoblotted with an antibody against VP2/VP3. (Right) Liposomes harboring His-tagged ERp29 were incubated with either BSA or Py and a lumenal extract. Samples were treated with proteinase K and Triton X-100 (where indicated) and immunoblotted with an antibody against the His-epitope.

(C) An ERp29-depleted extract was tested for membrane binding activity.

(D) A 3T6 cell extract overexpressing ERp29 was compared to a control extract for membrane binding activity.

(E) (left) Membrane binding activity of a virus containing only the VP1 protein (VP1-VLP) is compared to a wild-type (WT) Py. (right) The ability of VP1-VLP to generate the VP1b fragment was tested, as in Figure 1.

and the lumenal extract. Therefore the sensitivity of the membrane-associated virus to protease digestion reflects virus bound to the liposome surface, but not penetrated into its interior, where the virus would be largely protected from protease treatment.

We tested the ability of an ERp29-depleted extract to induce liposome binding and found that an ERp29-depleted extract caused substantially less VP1 to associate with liposomes than did an untreated control (Figure 5C, compare lane 4 to lane 2), demonstrating that ERp29 is required to induce Py virion binding. Moreover, treatment with an extract from cells overexpressing ERp29 increased liposome association of virions when compared to a control (Figure 5D, compare lane 4 to lane 2). These findings are consistent with the protease-digestion assay: an ERp29-depleted extract failed to induce VP1b formation and membrane binding, whereas a cell extract with overexpressed ERp29 stimulated these reactions compared to a control extract. Our data suggest that ERp29 renders Py virions hydrophobic, allowing the entire viral particle to bind to the surface of the ER membrane; this step may prepare the virus for penetration across the lipid bilayer.

Exposure of the hydrophobic surfaces of the internal VP2 and VP3 proteins of Py or the VP2 myristic acid may cause Py particles to bind liposomes and by inference to associate with the lumenal membrane of the ER. To test this possibility, we asked whether a virus-like particle consisting of only the VP1, but not the VP2 and VP3, proteins ("VP1-VLP") binds to the liposomes after being exposed to a lumenal extract. We found that in contrast to the wild-type Py, the VP1-VLP did not bind to the liposome after incubation with a lumenal extract (Figure 5E, compare lane 4 in left top and bottom panels), even though the addition of the lumenal extract to the VP1-VLP did generate the VP1b peptide (Figure 5E, right panel, compare lane 2 to lane 1). The observation that VP1-VLP does not bind to the liposomes implicates VP2 and/or VP3 in membrane binding.

ERp29 Facilitates Py Infection in the Intact Cell

Our in vitro protease-digestion and membrane binding assays suggest a role for ERp29 in the transport of Py from the ER into the cytosol, a step that occurs before the virus reaches the nucleus to replicate. To determine whether ERp29 plays a role in Py infection, we asked whether manipulating ERp29 activity affects viral infection. We monitored the expression of the virally encoded VP1 protein, an event that follows viral DNA transcription and replication in the nucleus, to assess Py infection efficiency.

To measure the appearance of newly synthesized

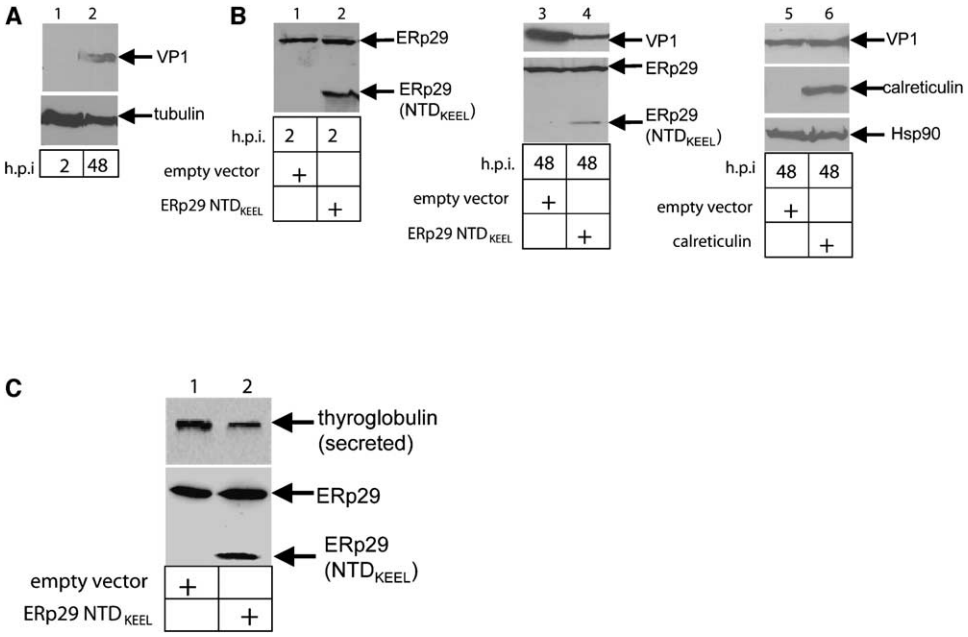

Figure 6. ERp29 Facilitates Py Infection

(A) 3T6 cells were incubated with Py for 2 hr, washed, and the cells were harvested or allowed to continue to grow for an additional 46 hr and then harvested. The lysates were probed for the presence of VP1 and tubulin as a loading control.

(B) As in (A) except, where indicated, cells were transfected with either an empty vector, a cDNA encoding ERp29 NTD_{KEEL}, or a cDNA encoding HA-tagged calreticulin, prior to infection. An antibody against HA was used to detect the expression of calreticulin. Hsp90 level was used as a loading control.

(C) FRTL-5 rat thyrocytes were transfected with either an empty vector or cDNA encoding ERp29 NTD_{KEEL}. The levels of ERp29, NTD (lower), and extracellular thyroglobulin (upper) were assessed by immunoblotting.

VP1 proteins, NIH 3T6 cells were incubated with Py for 2 hr, and the unbound virus was removed by washing with media. The cells were either harvested immediately or allowed to incubate for an additional 46 hr before the cells were harvested. We detected VP1 in lysates harvested at 48 hr, but not 2 hr, postinfection (Figure 6A, compare lane 2 to lane 1). The absence of VP1 in the 2 hr postinfection lysates indicates that the level of virus that entered the cells within this time frame is below the detection limit of the system. Hence, the appearance of VP1 in the 48 hr postinfection lysates represents newly synthesized VP1 and reflects successful infection.

Because the ERp29 NTD inhibited the generation of the VP1b fragment (Figure 4D), we asked whether expression of the NTD affects viral infection. The ER retention sequence KEEL at the C terminus of ERp29 was appended to the NTD (NTD_{KEEL}) to facilitate NTD retention in the ER. A cDNA encoding ERp29 NTD_{KEEL} was transiently transfected into 3T6 cells for 48 hr, and the cells were infected. Because Py arrives in the ER maximally 2–4 hr postinfection (Gilbert and Benjamin, 2004), the cells were either harvested 2 hr postinfection to examine the NTD_{KEEL} level or allowed to grow for an additional 46 hr to examine VP1 expression. In the 2 hr postinfection lysate, we found the NTD_{KEEL} and ERp29 levels to be similar in the NTD_{KEEL}-transfected lysate (Figure 6B, lane 2). At 48 hr postinfection, we found a decreased VP1 level in the ERp29 NTD_{KEEL}-transfected lysate when compared to a control lysate transfected with an empty vector (Figure 6B, top panel, compare lane 4 to lane 3). The lower NTD_{KEEL} level when compared to ERp29 is likely caused by dilution of the transfected cDNA 48 hr postinfection (Figure 6B, bottom panel, lane 4). As a control, overexpression of the hemagglutinin (HA)-tagged ER-resident protein, calreticulin (Figure 6B, middle panel, lane 6), did not decrease the VP1 level 48 hr postinfection (Figure 6B, top panel, compare lane 6 to lane 5).

Because ERp29 was initially found to mediate the secretion of thyroglobulin (Sargsyan et al., 2002), we asked whether NTD_{KEEL} overexpression also affects thyroglobulin secretion. Indeed, when the ERp29 NTD_{KEEL} was expressed in the FRTL-5 rat thyroid epithelial cells (Figure 6C, bottom panel, lane 2), the secreted thyroglobulin level in the media decreased moderately (Figure 6C, top panel, compare lane 2 to lane 1). These findings not only indicate that ERp29 NTD acts generally to inhibit endogenous ERp29 activity but, more importantly, demonstrate that ERp29 facilitates Py infection.

Discussion

Py travels from the plasma membrane to the ER from which it exits into the cytosol and then enters the nucleus to initiate infection. The physiological factor(s) in the ER that cause Py to transport across the ER membrane, as well as the molecular mechanism guiding this membrane penetration process, were largely unknown. Our results here identify an ER factor that induces a

conformational change in Py and provide mechanistic insight into how Py may breach the ER membrane.

ERp29 Triggers a Conformational Change in Py

By using a protease digestion assay, we first show that a conformational change is imparted upon Py by an activity in an ER lumenal extract. Mass-spectrometry demonstrated that the conformational change exposes the C-terminal arm of VP1; whether the N terminus of VP1 is exposed remains unclear. As the X-ray structure of polyomavirus shows that the N-terminal region of VP1 is close to the C-terminal invading arm of a neighboring VP1 (Stehle et al., 1994), it is possible that ERp29 also exposes that N-terminal region. Next, using an unbiased biochemical fractionation approach, we pinpointed ERp29, a structural homolog of PDI, as a potential candidate for the activity. Immunodepletion of ERp29 from the extract abolished activity, whereas overexpression of ERp29 in mammalian cells stimulated this reaction. Moreover, addition of ERp29's NTD, but not the CTD, to the extract inhibited activity. These findings establish ERp29 as a crucial component of ER activity that exposes the C-terminal arm of VP1.

Although not essential, the reductant DTT and the calcium-chelator EGTA stimulated the ER-induced Py conformational change. It is possible that DTT and EGTA partially destabilized Py's structure, enabling ERp29 to subsequently expose VP1's C-terminal arm efficiently. This explanation is supported by previous biochemical and X-ray structural studies showing that disulfide bridges and calcium ions provide critical structural support for Py (Brady et al., 1978; Stehle et al., 1996). Because the disulfide bond in Py virions is in proximity to the N terminus of VP1, its reduction may enable ERp29 to also expose the VP1 N terminus. DTT and EGTA likely mimicked the action of ER reductases (e.g., PDI) and calcium binding proteins (e.g., calnexin and calreticulin) that would normally act on the virus. In fact, downregulation of PDI in cells was recently observed to inhibit Py infection (J. Gilbert, W. Ou, J. Silver, and T.B., unpublished data).

The molecular mechanism by which the NTD acts to inhibit ERp29 activity is unclear. As the NTD mediates ERp29 homodimerization (Liepinsh et al., 2001), the NTD could disrupt the ERp29 homodimer through formation of an NTD:ERp29 heterodimer and, as a consequence, attenuate ERp29's activity. Whether ERp29 is sufficient to drive the Py conformational change remains uncertain, as purified, bacterially expressed ERp29 was inactive; the protein may be folded improperly, lack a posttranslational modification, or require additional ER factors to recapitulate the reaction. Further experiments will clarify these possibilities.

ERp29 and Membrane Penetration of Py

We next examined how the ERp29-induced conformational change facilitates Py transport across the ER membrane. Given its relatively large size (450 Å in diameter), even a partially disassembled Py particle is unlikely to transport across a protein-conducting channel in the ER membrane. We therefore postulate that Py penetrates the ER membrane by crossing the lipid bilayer directly. By using a liposome binding assay, we showed that incubation of Py with an ER lumenal extract stimulated the entire viral particle to bind to liposomes. This step presumably mimics binding of Py to the lumenal side of the ER membrane in preparation for its penetration across the bilayer. Similar to the protease digestion assay, we found that an ERp29-depleted extract was unable to promote liposome binding, whereas an extract from 3T6 cells overexpressing ERp29 stimulated this response. Thus, in addition to exposing the VP1 C-terminal arm, ERp29 also facilitates Py membrane binding.

Although the precise mechanism by which externalization of the VP1 C-terminal arm causes membrane binding remains unknown, our data implicate the involvement of Py's internal proteins VP2 and VP3, because a VLP consisting of only the VP1 shell does not bind liposomes. A possible scenario is that exposure of the VP1 C-terminal arm leads to an expansion of the central "pore" of the VP1 pentamer, enabling the VP2 myristic acid to emerge through the pore (Chen et al., 1998); the resulting hydrophobic viral particle then binds to the membranes. In fact, a mutant Py in which the VP2 lacks the myristic acid was shown previously to infect cells with 15-fold less efficiency, suggesting a role of the VP2 myristic acid in viral infection (Sahli et al., 1993).

ERp29-mediated externalization of the VP1 C-terminal arm and possibly the VP2 myristic acid is remarkably similar to the mechanism by which receptor interaction causes the nonenveloped poliovirus to bind to membranes. Upon binding to its receptor, poliovirus undergoes a conformational change accompanied by externalization of VP4 (which is myristoylated at its N terminus) and the N-terminal arm of VP1 (Fricks and Hogle, 1990). In fact, early studies have already shown that poliovirus binding to its receptor at the cell surface causes VP4 to exit from the viral particle (Lonberg-Holm et al., 1975; De Sena and Mandel, 1977). The ERp29-Py interaction is also reminiscent of the interaction between cellular proteases and the nonenveloped reovirus: proteolytic processing of reovirus triggers the exposure of the hydrophobic, N terminally myristoylated μ1N peptide, generating a hydrophobic particle that allows it to bind and penetrate the late endosomal membrane (Chandran and Nibert, 2003).

How the membrane-embedded Py reaches the cytosol is unknown. The virus-membrane interaction could induce holes in the bilayer by disrupting the phospholipid organization, thereby enabling the virus to "squeeze" through the holes. The "leakiness" of the ER membrane (Le Gall et al., 2004) due to its low cholesterol concentration may be a membrane property that further facilitates Py's penetration process. Spontaneous partitioning of the membrane-embedded hydrophobic virus into the aqueous cytosolic environment is unfavorable energetically. Thus, it is conceivable that cytosolic chaperones would bind to the exposed hydrophobic regions of Py on the cytosolic surface of the ER membrane and extract the virus into the cytosol. This situation is similar to the role of the cytosolic p97 ATPase in extracting misfolded ER proteins from the ER membrane into the cytosol (Ye et al., 2001).

The Role of ERp29 in Py Infection

To establish a functional role of ERp29 in Py infection, we demonstrated that in the intact cell, overexpression of the dominant-negative ERp29 NTD reduced the efficiency of viral infection. This finding indicates that the Py conformational change imparted by ERp29 is a critical event leading to successful viral infection.

PDI-Family Members: A General Class of ER Remodeling Chaperones?

We previously demonstrated that PDI unfolds CT (Tsai et al., 2001). Here, the PDI-like protein ERp29 is shown to trigger a conformational change in Py. The striking observation that PDI-like proteins mediate these reactions implicates PDI family members as a general class of ER remodeling chaperones.

It is unlikely that the remodeling activities displayed by PDI and ERp29 are intended to mediate pathogen entry, but more likely represent reactions crucial for normal cellular functions. For instance, unfolding events in the ER initiate the translocation of misfolded proteins from the ER to the cytosol for degradation by the proteasome, a process called retrotranslocation (Tsai et al., 2002). CT disguises itself as a misfolded substrate to hijack this translocation process and reach the cytosol (Hazes and Read, 1997). In fact, in addition to facilitating CT retro-translocation, PDI has been shown to play a similar role for misfolded ER substrates (Molinari et al., 2002). The parallel cellular function of ERp29's remodeling activity remains to be characterized.

What are the energy sources that drive both PDI and ERp29's remodeling reactions? PDI family members are characterized by the presence of a thioredoxin domain in their structures. Within this domain is the signature CxxC motif that allows the protein to cycle between a reduced and an oxidized state. In some cases, one of the Cys residues is replaced by a different residue (e.g., CxxA). PDI has four thioredoxin domains, two of which contain the CxxC motif. We found previously that PDI's redox states drive its unfolding activity (Tsai et al., 2001): in its reduced state, PDI binds and unfolds the toxin, whereas in its oxidized state, PDI releases it. That PDI acts as a redox-driven chaperone was observed in the retro-translocation of the membrane protein BACE457 (Molinari et al., 2002). Because ERp29 contains only a single Cys residue in its entire sequence (Cys157), it remains either in the reduced state or forms a mixed-disulfide with another ER factor. Thus ERp29's reduced and mixed-disulfide bonded states may exhibit different conformations, enabling it to bind to substrates with different affinities. Alternatively, noncovalent interactions with other ER factors could change ERp29's conformation to drive the substrate binding and release cycle.

Experimental Procedures

Materials

Py and VP1 antibodies were provided by the Benjamin laboratory. Antibodies against the VP2/VP3 proteins and the VP1 VLP were generous gifts from Dr. Roberto Garcea (University of Colorado). Monoclonal antibodies against rat ERp29 were produced by ASLA BIOTECH Ltd. (Riga, Latvia). Polyclonal antibodies against rat thyroglobulin were a gift from Dr. B. Di Jeso (University of Lecce, Italy). Microsomes from dog pancreas were a generous gift from Dr. Tom Rapoport (Harvard Medical School). Purified phospholipids were purchased from Avanti.

Fractionation of ER Lumenal Extract from Dog Pancreas Microsomes

An ER lumenal extract derived from dog pancreas microsomes was prepared as before (Tsai et al., 2001). The extract was bound to a Con A-Sepharose column and the flow-through was collected and bound to the weak anion exchange DEAE-Sepharose column. Next, the flow-through proteins from this column were bound to the strong anion exchange Q-Sepharose column, and the bound proteins were eluted from the column with an increasing salt gradient (50 mM to 1M potassium acetate). 0.5 ml fractions were collected, dialyzed, and analyzed for both their protein content and their ability to generate the VP1b peptide.

Preparation of a Cytosolic Extract

3T6 cells were incubated with 0.025% digitonin for 10 min at 4°C to selectively permeabilize the plasma membrane, but not internal organelle membranes (Le Gall et al., 2004). Cells were centrifuged at 14,000 rpm for 10 min at 4°C to "squeeze" out the cytosolic content. SDS-PAGE analysis followed by immunoblotting revealed the cytosolic extract did not contain ER proteins (Figure 2).

Trypsin Sensitivity Assay

Py was incubated with or without DTT (3 mM) and EGTA (10 mM) for 20 min at 37°C. BSA (1 mg/ml), a lumenal extract (1mg/ml), or a cytosolic extract (1 mg/ml) was added to the sample and incubated for 60 min at 37°C. Trypsin (0.25 mg/ml) was added to the samples for 30 min at 4°C, and the reaction was stopped by the addition of TLCK (1 mM) for 10 min at 4°C. Samples were analyzed by reducing SDS-PAGE followed by immunoblotting with a VP1 antibody.

Identification of the VP1b Fragment

The VP1b fragment is generated by incubating Py in the presence of DTT (3 mM), EGTA (10 mM), and a lumenal extract, followed by trypsin addition (0.25 mg/ml). To facilitate isolation of the VP1b fragment, we found that Py incubated in the presence of DTT (3 mM), EGTA (10 mM), and a higher concentration of trypsin (5 mg/ml) also generated the VP1b fragment. Full-length VP1 and VP1b fragments were excised from an SDS-PAGE gel and subjected to mass-spectroscopy analysis. Results demonstrated that a tryptic-peptide (VYDGTEPVPGDPDMTR) corresponding to residues 353–368 in VP1 is absent in VP1b, suggesting that VP1b represents residues 1–352 of VP1. The position of residue R352 in the existing structure of the Py VP1 pentamer (PDB number 1sid; Stehle et al., 1994) is highlighted in Figure 1D.

Immunodepletion of ERp29

50 μl of an ER lumenal extract was incubated with an ERp29, a PDI, or an Ero1 antibody overnight at 4°C, followed by adding 20 μl of protein A Sepharose beads.

Heterologous Expression and Purification of Rat ERp29 NTD and CTD

cDNA fragments encoding ERp29 NTD (residues 33–154) and CTD (residues 155–260) were generated by PCR amplification and subcloned into pQE30. The constructs were transformed into BL21 *E. coli*. Single colonies were picked and used to inoculate a 5 ml LB overnight culture. The culture was diluted into 500 ml LB and grown to OD_{600} = 0.3. IPTG (1 mM) was added to the culture, which was then allowed to grow for 2 hr. Cells were pelleted, resuspended in a lysis buffer (150 mM KOAc, 250 mM sucrose, 50 mM HEPES [pH 7.5], 2 mM $Mg(OAc)_2$, 1% Triton X-100, and protease inhibitors), dounced, and sonicated. The cell debris was pelleted, and the resulting supernatant containing NTD or CTD was purified by binding to a Qiagen Ni-NTA Agarose column and elution with imidazole (150 mM). The proteins were dialyzed and analyzed for purity by Coomassie staining.

Liposome Binding Assay

Biotinylated-liposome was made by mixing chloroform-dissolved phosphatidyl-choline (80 μg), -ethanolamine (25 μg), -inositol (12.5 μg), -serine (3 μg), and biotinylated-phosphatidyl-ethanolamine (25 μg). The mixture was dried, resuspended in a buffer (50 mM HEPES [pH7.6], 250 mM sucrose, 150 mM KOAc, and 2 mM $MgCl_2$) with or without purified His-tagged ERp29 (5 μg), and sonicated. Strepavidin-coated magnetic beads were added to the liposomes and transferred to a magnetic apparatus to pellet the biotinylated-liposomes. To analyze Py binding, Py was incubated with the indicated extract for 60 min at 37°C, then incubated with the biotinylated-liposomes bound to Strepavidin-coated magnetic beads for 20 min at 37°C and transferred to a magnetic apparatus to pellet the biotinylated-liposomes and any membrane bound material. Both the pellet and supernatant fractions were subjected to SDS-PAGE, followed by immunoblotting with a VP1 or VP2/3 antibodies. Where indicated, samples were treated with 0.1 mg/ml of proteinase K for 30 min at 4°C prior to SDS-PAGE analysis.

Infection Assay

NIH-3T6 cells were plated in 6-well dishes. Where indicated, cells were transfected with a cDNA construct encoding rat ERp29 NTD_{KEEL}(pcDNA3.1-ERp29NTD_{KEEL}). The ERp29 NTD_{KEEL} construct was generated by appending ERp29's KEEL sequence to residue M154 of the NTD. 48 hr posttransfection, cells were washed and infected with Py. After 2 hr, the cells were washed to remove extracellular virus and either harvested or allowed to incubate for 46 additional hrs at which point the cells were harvested. Cells were lysed, subjected to SDS-PAGE, and immunoblotted with antibodies against VP1, ERp29, an HA-epitope, Hsp90, or tubulin.

Thyroglobulin Secretion

FRTL-5 rat thyrocytes were transfected with pcDNA3.1-ERp29NTD_{KEEL}. 48 hr after transfection, the medium was collected, centrifuged for 20 min at 17,000 × g, and the supernatant was analyzed for the presence of thyroglobulin. Cells were lysed, centrifuged for 10 min at 17,000 × g, and the supernatant was analyzed for the presence of ERp29 and NTD.

Acknowledgments

We thank Tom Rapoport and Kristen Verhey for critically reading the manuscript. B.T. is a Biological Scholar at the University of Michigan Medical School. E.K.R. is supported by a training grant from the National Science Foundation. S.M. was supported by the Swedish Medical Research Council and the Swedish Society of Medicine. M.B. received a scholarship from the Royal Swedish Academy. The work was supported in part by a grant to T.B. from the National Cancer Institute (CA 082395).

Received: May 12, 2005
Revised: July 28, 2005
Accepted: August 31, 2005
Published: October 27, 2005

References

Brady, J.N., Winston, V.D., and Consigli, R.A. (1978). Characterization of a DNA-protein complex and capsomere subunits derived from polyoma virus by treatment with ethyleneglycol-bis-N,N′-tetraacetic acid and dithiothreitol. J. Virol. *27*, 193–204.

Chandran, K., and Nibert, M.L. (2003). Animal cell invation by a large nonenveloped virus: reovirus delivers the goods. Trends Microbiol. *11*, 374–382.

Chandran, K., Farsetta, D.L., and Nibert, M.L. (2002). Strategy for nonenveloped virus entry: a hydrophobic conformer of the reovirus membrane penetration protein micro 1 mediates membrane disruption. J. Virol. *76*, 9920–9933.

Chen, X.S., Stehle, T., and Harrison, S.C. (1998). Interaction of polyomavirus internal protein VP2 with the major capsid protein VP1 and implications for participation of VP2 in viral entry. EMBO J. *17*, 3233–3240.

Clissold, P.M., and Bicknell, R. (2003). The thioredoxin-like fold: hidden domains in protein disulfide isomerases and other chaperone proteins. Bioessays *25*, 603–611.

De Sena, J., and Mandel, B. (1977). Studies on the in vitro uncoating of poliovirus. II. Characteristics of the membrane-modified particle. Virology *78*, 554–566.

Fricks, C.E., and Hogle, J.M. (1990). Cell-induced conformational change in poliovirus: externalization of the amino terminus of VP1 is responsible for liposome binding. J. Virol. *64*, 1934–1945.

Gilbert, J., and Benjamin, T. (2004). Uptake pathway of polyomavirus via ganglioside GD1a. J. Virol. *78*, 12259–12267.

Hazes, B., and Read, R.J. (1997). Accumulating evidence suggests that several AB-toxins subvert the endoplasmic reticulum-associated protein degradation pathway to enter target cells. Biochemistry *36*, 11051–11054.

Kartenbeck, J., Stukenbrok, H., and Helenius, A. (1989). Endocytosis of simian virus 40 into the endoplasmic reticulum. J. Cell Biol. *109*, 2721–2729.

Le Gall, S., Neuhof, A., and Rapoport, T. (2004). The endoplasmic reticulum membrane is permeable to small molecules. Mol. Biol. Cell *15*, 447–455.

Liepinsh, E., Baryshev, M., Sharipo, A., Ingelman-Sundberg, M., Otting, G., and Mkrtchian, S. (2001). Thioredoxin fold as homodimerization module in the putative chaperone ERp29: NMR structures of the domains and experimental model of the 51 kDa dimer. Structure *9*, 457–471.

Lonberg-Holm, K., Gosser, L.B., and Kauer, J.C. (1975). Early alteration of poliovirus in infected cells and its specific inhibition. J. Gen. Virol. *27*, 329–345.

Mkrtchian, S., Fang, C., Hellman, U., and Ingelman-Sundberg, M. (1998). A stress-inducible rat liver endoplasmic reticulum protein, ERp29. Eur. J. Biochem. *251*, 304–313.

Molinari, M., Galli, C., Piccaluga, V., Pieren, M., and Paganetti, P. (2002). Sequential assistance of molecular chaperones and transient formation of covalent complexes during protein degradation from the ER. J. Cell Biol. *158*, 247–257.

Nakanishi, A., Clever, J., Yamada, M., Li, P.P., and Kasamatsu, H. (1996). Association with capsid proteins promotes nuclear targeting of simian virus 40 DNA. Proc. Natl. Acad. Sci. USA *93*, 96–100.

Norkin, L.C., Anderson, H.A., Wolfrom, S.A., and Oppenheim, A. (2002). Caveolar endocytosis of simian virus 40 is followed by brefeldin A-sensitive transport to the endoplasmic reticulum, where the virus disassembles. J. Virol. *76*, 5156–5166.

Pelkmans, L., and Helenius, A. (2003). Insider information: what viruses tell us about endocytosis. Curr. Opin. Cell Biol. *15*, 414–422.

Pelkmans, L., Kartenbeck, J., and Helenius, A. (2001). Caveolar endocytosis of simian virus 40 reveals a new two-step vesicular transport pathway to the ER. Nat. Cell Biol. *3*, 473–483.

Poranen, M.M., Daugelavicius, R., and Bamford, D.H. (2002). Common principles in viral entry. Annu. Rev. Microbiol. *56*, 521–538.

Richards, A.A., Stang, E., Pepperkok, R., and Parton, R.G. (2002). Inhibitors of COP-mediated transport and cholera toxin action inhibit simian virus 40 infection. Mol. Biol. Cell *13*, 1750–1764.

Sahli, R., Freund, R., Dubensky, R., Garcea, R., Bronson, R., and Benjamin, T.L. (1993). Defect in entry and altered pathogenicity of a polyoma virus mutant blocked in VP2 myristylation. Virology *192*, 142–153.

Sargsyan, E., Baryshev, M., Szekely, L., Sharipo, A., and Mkrtchian, S. (2002). Identification of ERp29, an endoplasmic reticulum lumenal protein, as a new member of the thyroglobulin folding complex. J. Biol. Chem. *277*, 17009–17015.

Schmitz, A., Herrgen, H., Winkeler, A., and Herzog, V. (2000). Cholera toxin is exported from microsomes by the Sec61p complex. J. Cell Biol. *148*, 1203–1212.

Skehel, J.J., and Wiley, D.C. (2000). Receptor binding and membrane fusion in virus entry: the influenza hemagglutinin. Annu. Rev. Biochem. *69*, 531–569.

Smith, A.E., and Helenius, A. (2004). How viruses enter animal cells. Science *304*, 237–242.

Stehle, T., Yan, Y., Benjamin, T.L., and Harrison, S.C. (1994). Structure of murine polyomavirus complexed with an oligosaccharide receptor fragment. Nature *369*, 160–163.

Stehle, T., Gamblin, S.J., Yan, Y., and Harrison, S.C. (1996). The structure of simian virus 40 refined at 3.1 A resolution. Structure *4*, 165–182.

Streuli, C.H., and Griffin, B.E. (1987). Myristic acid is coupled to a structural protein of polyoma virus and SV40. Nature *326*, 619–622.

Tsai, B., Rodighiero, C., Lencer, W.I., and Rapoport, T.A. (2001). Protein disulfide isomerase acts as a redox-dependent chaperone to unfold cholera toxin. Cell *104*, 937–948.

Tsai, B., Ye, Y., and Rapoport, T. (2002). Retro-translocation of proteins from the endoplasmic reticulum into the cytosol. Nat. Rev. Mol. Cell Biol. *3*, 246–255.

Tsai, B., Gilbert, J.M., Stehle, T., Lencer, W.I., Benjamin, T.L., and Rapoport, T.A. (2003). Gangliosides are receptors for murine polyoma virus and SV40. EMBO J. *22*, 4346–4355.

Ye, Y., Meyer, H.H., and Rapoport, T.A. (2001). The AAA ATPase Cdc48/p97 and its partners transport proteins from the ER into the cytosol. Nature *414*, 652–656.